International Immunopharmacology 75 (2019) 105834

Contents lists available at ScienceDirect

International Immunopharmacology

journal homepage: www.elsevier.com/locate/intimp

Transforming growth factor-β1 and hypoxia inducible factor-1α synergistically inhibit the osteogenesis of periodontal ligament stem cells

Zhihua Liu[a], Ling Guo[a], Rulei Li[a], Qian Xu[b], Jiajia Yang[c], Jinyi Chen[d], Manjing Deng[a,*]

[a] Department of Stomatology, Daping Hospital & Research Institute of Surgery, Army Medical University, Chongqing 400042, China
[b] Department of Stomatology, Children's Hospital of Chongqing Medical University, Chongqing 400014, China
[c] Department of Stomatology, People's Hospital of Tongnan District, Chongqing 402660, China
[d] Department of Dermatology, Daping Hospital & Research Institute of Surgery, Army Medical University, Chongqing 400042, China

ARTICLE INFO

Keywords:
Mesenchymal stem cell
Osteogenesis
Hypoxia inducible factor-1α
Transforming growth factor-β1
Mothers against decapentaplegic homolog 3

ABSTRACT

Periodontal ligament stem cells (PDLSCs) exhibit potential for osteogenesis in vitro and in vivo and are a candidate cell type for periodontal regeneration for the treatment of periodontitis. However, periodontitis is accompanied by hypoxia, and it is not clear how hypoxia affects the osteogenesis of PDLSCs. In this study, we found that the expression of hypoxia-inducible factor-1α (HIF-1α) and transforming growth factor-β1 (TGF-β1) is enhanced in the osteogenesis of PDLSCs under nonhypoxic conditions. TGF-β1 can induce the stabilization of HIF-1α through the phosphorylation of mothers against decapentaplegic homolog 3 (Smad3) in PDLSCs, and in turn, HIF-1α inhibits the mRNA and protein expression of TGF-β1 and inhibits the phosphorylation of Smad3 in PDLSCs. In addition, both HIF-1α and TGF-β1 reduce the expression of crucial osteogenic gene runt-related transcription factor 2 (RUNX2) and the mineralization of PDLSCs in normoxia. In conclusion, our results showed that TGF-β1 can induce the stabilization of HIF-1α in PDLSCs under nonhypoxic conditions, that HIF-1α can negatively regulate the TGF-β1/Smad3 signal pathway in PDLSCs, and that TGF-β1 and HIF-1α can synergistically inhibit the osteogenesis of PDLSCs.

1. Introduction

Periodontitis is a prevalent chronic inflammatory disease that affects supporting periodontal tissues [1]. Typical therapies for periodontitis, including scaling and root planning (SRP), medication, and the newly adopted photodynamic therapy (PDT) method [2,3] can block inflammatory progression and rehabilitate lost attachment levels to some extent, but alveolar bone lost cannot be recovered satisfactorily. Periodontal ligament stem cells (PDLSCs) were first isolated and characterized by Seo et al. in 2004 and exhibited the potential for osteogenic and chondrogenic differentiation in vitro, forming cement- or periodontal ligament-like tissues in vivo [4], thus constituting feasible and promising tools for recovering lost alveolar bone in treating periodontitis.

Periodontitis is accompanied by hypoxia with oxygen saturation being decreased from 77% to 71% [5]. Hypoxia-inducible factor-1 (HIF-1) is a critical transcription factor in response to lowered oxygen levels [6,7] and is composed of constitutional component HIF-1β and active subunit HIF-1α, which functions as the master hypoxia sensor [8]. Hypoxia can affect osteogenic progression via HIF-1α. On one hand, after applying a virus encoding HIF-1α genes in combination with a gelatin scaffold carrier, the formation of new bones and vessels has been observed in a rat alveolar bone defect model [9]. On the other hand, however, HIF-1α has been found to induce a reduction in runt-related transcription factor 2 (RUNX2) and osterix (OSX) in human periodontal ligament cells (PDLCs) through extracellular signal-regulated kinase 1/2 (ERK1/2), c-Jun N-terminal kinase (JNK), and p38 mitogen-activated protein kinase (MAPK) pathways [10]. Furthermore, cobalt chloride ($CoCl_2$)-induced HIF-1α can induce the reduction of osteogenic genes, e.g., *RUNX2* and alkaline phosphatase (*ALP*), in PDLCs [11,12]. Taken together, it could be inferred that bifunctional HIF-1α participates in the regulation of osteogenesis, and the molecular mechanisms of HIF-1α that shape the osteogenesis of PDLSCs are still not fully understood.

HIF-1α can be induced under hypoxia and nonhypoxic conditions. As was reviewed by Semenza, growth factors and cytokines can induce the expression of HIF-1α under nonhypoxic conditions [13]. Among them, TGF-β1 modulates skeletal development and bone homeostasis via mothers against decapentaplegic homolog (Smad) complex or MAPK pathways [14]. Watanabe et al. further proved that TGF-β1 can maintain the stabilization of HIF-1α under nonhypoxic conditions through the inhibition of prolyl hydroxylase 2 (PHD2) in PDLCs [15]. Yamazaki et al. also demonstrated that

* Corresponding author at: Department of Stomatology, Daping Hospital & Research Institute of Surgery, Army Medical University, 10 Changjiang Branch Road, Yuzhong District, Chongqing 400042, China.
E-mail address: dengmanjing@tmmu.edu.cn (M. Deng).

https://doi.org/10.1016/j.intimp.2019.105834
Received 24 March 2019; Received in revised form 11 August 2019; Accepted 17 August 2019
Available online 26 August 2019
1567-5769/ © 2019 Elsevier B.V. All rights reserved.

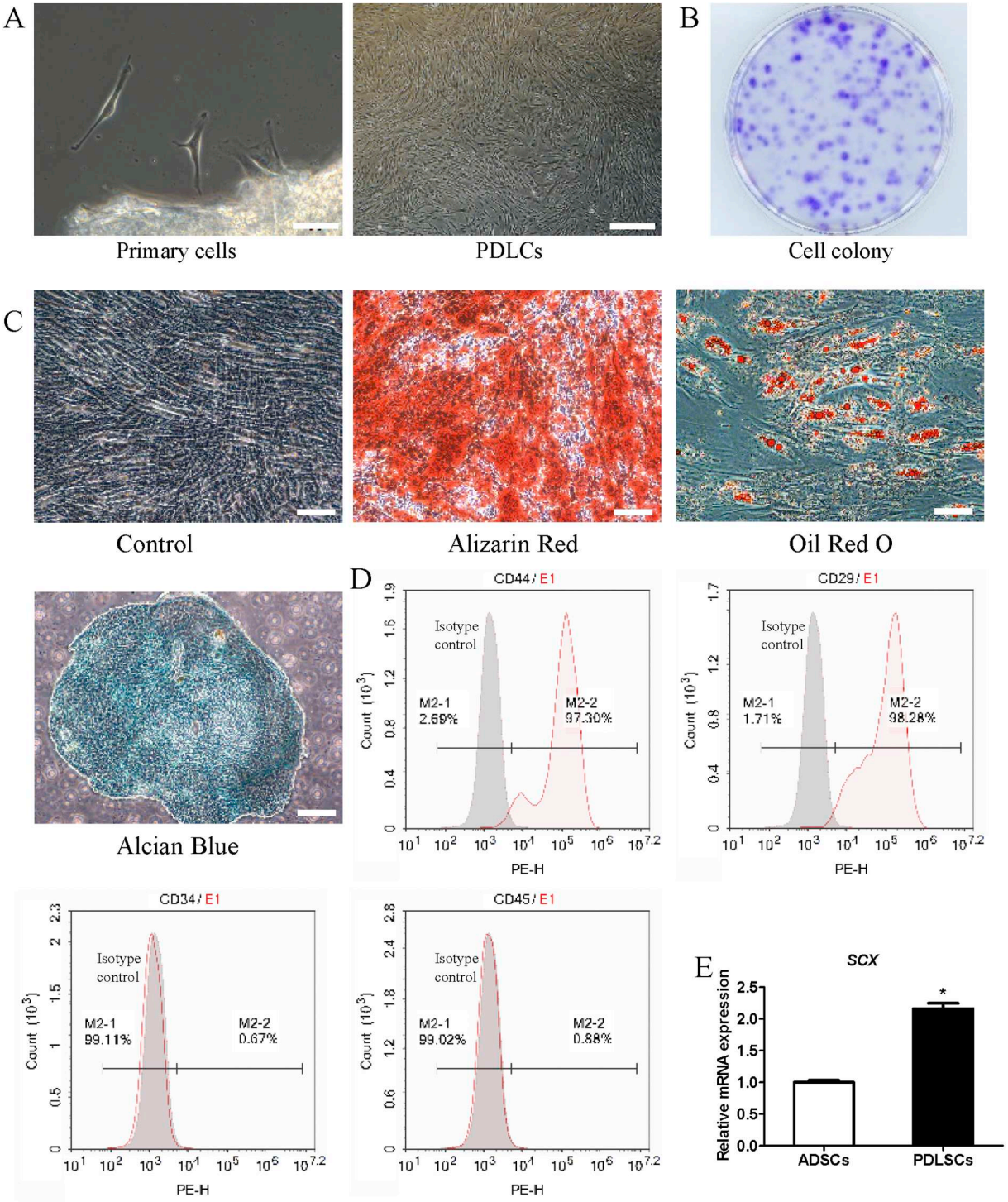

Fig. 1. Isolation and characterization of human PDLSCs. (A) Isolation and culturing of primary periodontal ligament cells. Spindle shaped cells appeared from the primary explants (scale bar = 50 μm) and reached a confluence level of 80% before passage (scale bar = 500 μm). (B) Single-cell colony formation assay and crystal violet staining. Experiments were carried out three times ($n = 2$). (C) Differentiation potential analysis by Alizarin Red S, Oil Red O and Alcian Blue staining (scale bar = 100 μm). Experiments were carried out three times ($n = 3$). (D) Flow cytometry analysis of stem cell surface markers CD44, CD29, CD34 and CD45 with the isotype control. Experiments were carried out three times ($n = 3$). (E) The expression of *SCX* in PDLCs was detected by qPCR relative to human adipose-derived stem cells (ADSCs). $^*p < .05$ versus the ADSC group. Experiments were carried out three times (n = 3). Donor is #1 (male and 14 years of age) and #15 (female and 18 years of age). (For interpretation of the references to color in this figure legend, the reader is referred to the web version of this article.)

TGF-β1 can induce the expression of HIF-1α in fibroblasts [16]. However, it has been reported that TGF-β1 does not influence the expression of HIF-1α in liver cancer HepG2 cells [17] or in human umbilical vein endothelial cells [18]. Thus, it could be assumed that the interrelationship between TGF-β1 and HIF-1α is context-dependent and that the role of TGF-β1 and HIF-1α in the osteogenesis of PDLSCs requires further study.

Taken together, we propose the hypothesis that TGF-β1 maintains the stabilization of HIF-1α in PDLSCs under nonhypoxic conditions and affects the osteogenesis of PDLSCs and the rehabilitation of alveolar bone by inducing the expression of HIF-1α. We believe that exploring modulation patterns between TGF-β1 and HIF-1α and underlying mechanisms would help further elucidate molecular networks of the

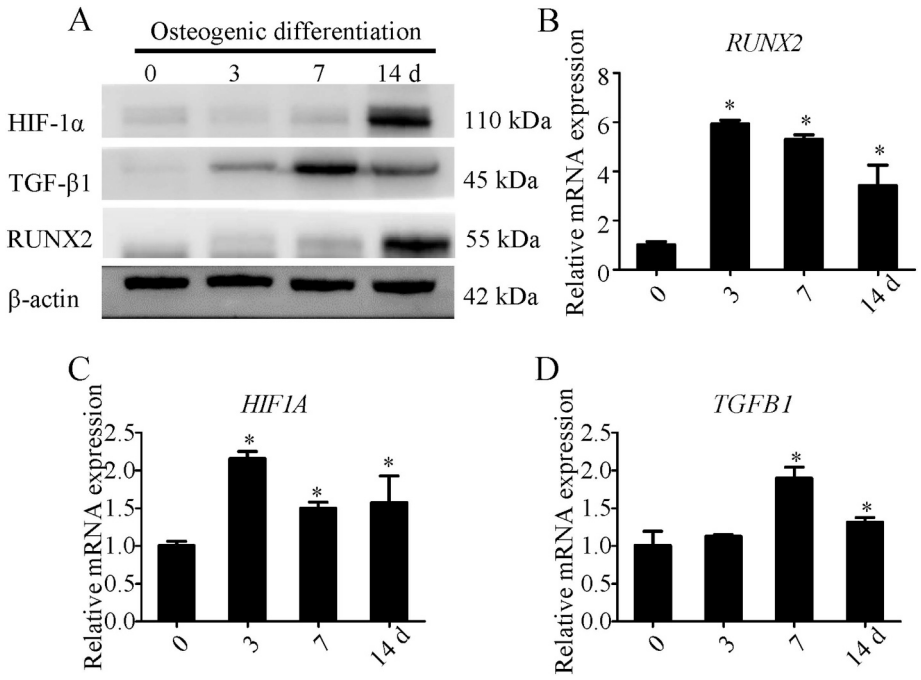

Fig. 2. Expression of HIF-1α and TGF-β1 during the osteogenesis of PDLSCs. (A-D) The mRNA and protein expression of HIF-1α, TGF-β1 and RUNX2 during the ordinary osteogenic differentiation of PDLSCs. ANOVA coupled with Dunnett's test (2-sided) was used to draw post-hoc comparisons. *$p < .05$ versus the control group. Experiments were carried out four times (n = 3). Donor is #7 (female and 13 years of age).

osteogenesis of PDLSCs and facilitate periodontal tissue regeneration for the treatment of periodontitis.

2. Material and methods

2.1. Isolation and characterization of PDLSCs

With approval from the Medical Ethics Committee of Daping Hospital of Army Medical University and with the informed written consent of the patients and their parents, healthy premolars were collected from 16 patients (12–18 years of age) undergoing orthodontic treatment at Daping Hospital. The middle third of each PDL was dissociated with 3 mg/ml type I collagenase (Sigma-Aldrich, Saint Louis, Missouri, USA) and 4 mg/ml dispase (Sigma-Aldrich, Saint Louis, Missouri, USA) for 1 h at 37 °C and then transferred to a 6-well plate containing α-minimum essential medium (α-MEM) (HyClone Laboratories, Logan, Utah, USA) with 10% fetal bovine serum (ExCell Bio, Taicang, Jiangsu, China), 100 U/ml penicillin and 100 mg/ml streptomycin (Solarbio, Beijing, China). Cover slides were carefully applied. The plate was then incubated at 37 °C in a humidified atmosphere containing 5% CO_2 (Thermo Fisher Scientific, Waltham, Massachusetts, USA). The culture medium was refreshed every 2 days. Putative stem cells were then purified by single-cell colony formation assay and stained with crystal violet dye (Beyotime, Shanghai, China). Only cells at passages 2–4 were used.

The differentiation potential of the putative stem cells was analyzed. Cells were plated in 6-well plates at a density of 10,000 cells/cm^2. Osteogenic medium was composed of basal medium supplemented with 50 μg/ml L-ascorbic-2-phosphate, 0.1 μmol/l dexamethasone, and 10 mmol/l β-glycerophosphate (all from Sigma-Aldrich, Saint Louis, Missouri, USA). Media was changed every 3 days. After 3 weeks of culture, cells were stained with 2% Alizarin Red S (pH 4.2) (Sigma-Aldrich, Saint Louis, Missouri, USA). Adipogenic induction medium was composed of: basal medium supplemented with 200 μmol/l indomethacin, 0.5 mmol/l 3-isobutyl-1-methylxanthine, 10 μmol/l insulin, and 1 μmol/l dexamethasone (all from Sigma-Aldrich, Saint Louis, Missouri, USA). Adipogenic maintenance medium was composed of the same reagents without 3-isobutyl-1-methylxanthine. After adipogenic induction for 1 day, adipogenic maintenance was performed for 3 days. After 4 weeks of culture, cells were stained with 0.3% Oil Red O (Sigma-Aldrich, Saint Louis, Missouri, USA). Chondrogenic medium was composed of: basal medium supplemented with 0.1 μmol/l dexamethasone, 0.05 μg/ml L-ascorbic-2-phosphat, 1% insulin-transferrin-selenium solution (all from Sigma-Aldrich, Saint Louis, Missouri, USA), and 0.01 μg/ml TGF-β3 (PeproTech, Rocky Hill, New Jersey, USA). Cells were pelleted in a 15 ml conical tube. After maintaining for 28 days, pellets were fixed in 4% paraformaldehyde, embedded in paraffin and sectioned. Then pellets were stained with Alcian Blue (Sigma-Aldrich, Saint Louis, Missouri, USA).

The expression of mesenchymal stem cell (MSC)-associated surface markers was analyzed by flow cytometry. Cells in the third passage (1.0×10^6 cells) were incubated with specific antibodies for CD34, CD45, CD44, CD29, and isotype control for 1 h at room temperature. All antibodies were purchased from BD Biosciences (Franklin Lakes, New Jersey, USA). The percentage of CD44-, CD29-, CD34-, and CD45-positive cells present was calculated using a BD FACSCalibur Flow Cytometer, and the results were analyzed using BD CellQuest Pro software (all from BD Biosciences, Franklin Lakes, New Jersey, USA).

Detection of scleraxis (SCX) expression. SCX is a transcription factor specifically expressed in tendon cells. Primer sequences of *SCX* mRNA for qPCR detection were set as follows: forward: AACAGATCTGCACC TTCTGCC, reverse: CGAATCGCTGTCTTTCTGTCG.

2.2. Hypoxia

Hypoxia was induced by exposing cells to a tri-gas incubator with 3% O_2 (Heal Force, Shanghai, China). Cobalt chloride ($CoCl_2$, 100 μmol/l; Sigma-Aldrich, Saint Louis, Missouri, USA) was used to induce the stabilization of HIF-1α protein. 3-(5′-hydroxymethyl-2′-furyl)-1-benzyl indazole (YC-1, 10 μmol/l; Sigma-Aldrich, Saint Louis, Missouri, USA), or BAY87–2243 (Selleck, Shanghai, China) were adopted to antagonize the effects of HIF-1α.

2.3. Osteogenesis assay

PDLSCs (passage 3) were plated in 24-well plates at a density of 10,000 cells/cm^2. The osteogenic composition of the medium used is described in Section 2.1. Osteogenic media were refreshed every 3 days. After the first day, total RNA were extracted for RUNX2 detection by qPCR. After 2 weeks, the plates were stained with 2% Alizarin Red S (pH 4.2) (Sigma-Aldrich, Saint Louis, Missouri, USA). The results were then digitalized with Image-Pro Plus (Media Cybernetics, Rockville, Maryland, USA).

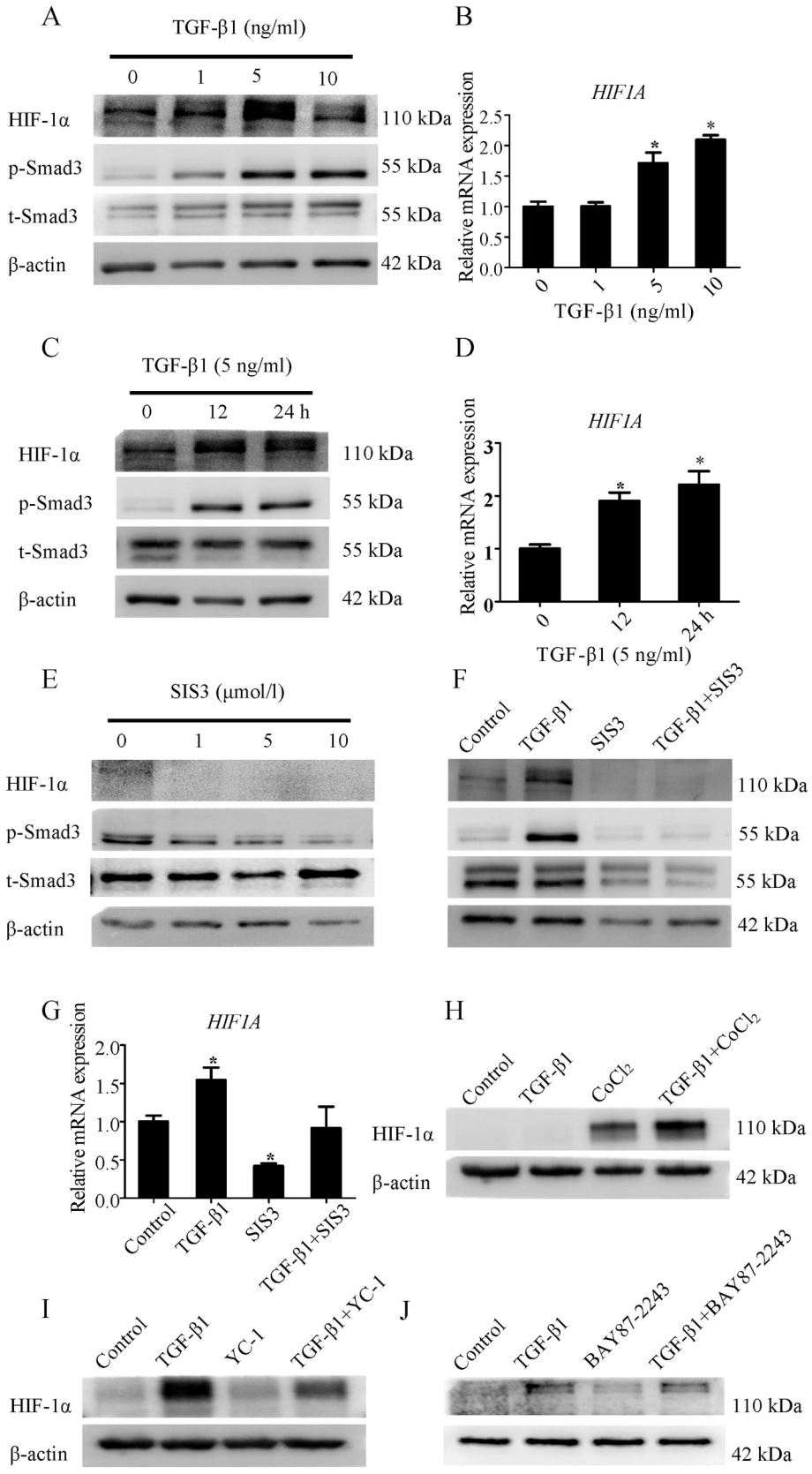

Fig. 3. TGF-β1 stabilizes HIF-1α expression in normoxia and enhances HIF-1α expression in hypoxia. After serum starving the culture for 24 h, different treatments were applied for 24 h. (AB) Dose-dependent TGF-β1 treatment (0, 1, 5 and 10 ng/ml) effects on the expression of HIF proteins and mRNA. ANOVA coupled with Dunnett's test (2-sided) was used to draw post hoc comparisons. *$p < .05$ versus the control group. (CD) Time-dependent TGF-β1 treatment (5 ng/ml for 0, 12 and 24 h) for the expression of HIF protein and mRNA. ANOVA coupled with Dunnett's test (2-sided) was used to draw post hoc comparisons. *$p < .05$ versus the control group. (E) Different concentrations of SIS3 (0, 1, 5 and 10 μmol/l) used for the expression of HIF proteins. (FG) PDLSCs were treated with TGF-β1, SIS3, or TGF-β1 + SIS3. TGF-β1 = 5 ng/ml, SIS3 = 10 μmol/l. ANOVA coupled with Bonferroni's correction was used to draw post hoc comparisons. *$p < .05$ versus the other groups. (H) PDLSCs were treated with TGF-β1, $CoCl_2$, or TGF-β1 + $CoCl_2$. $CoCl_2$ = 100 μmol/l. (I) PDLSCs were treated with TGF-β1, YC-1, or TGF-β1 + YC-1. YC-1 = 10 μmol/l. (J) PDLSCs were treated with TGF-β1, BAY87–2243, or TGF-β1 + BAY87-2243. BAY87-2243 = 100 μmol/l. t-Smad3 = total Smad3 protein, p-Smad3 = phosphorylated Smad3 protein. Experiments were carried out three times ($n = 3$). Donor is #6 (female and 16 years of age).

2.4. Western blot

Total protein was extracted using ice-cold lysis buffer composed of 10% RIPA (Solarbio, Beijing, China) and protease inhibitor cocktail (Roche, Basel, Switzerland). After centrifugation at 12000 ×*g* at 4 °C for 10 min with Heraeus Multifuge X1R (Thermo Fisher Scientific, Waltham, Massachusetts, USA), the supernatants were collected and protein concentrations were determined using a BCA Protein Assay Kit (Solarbio, Beijing, China). Samples were mixed with 5× sample loading buffer (Beyotime, Shanghai, China) and dry heated at 100 °C

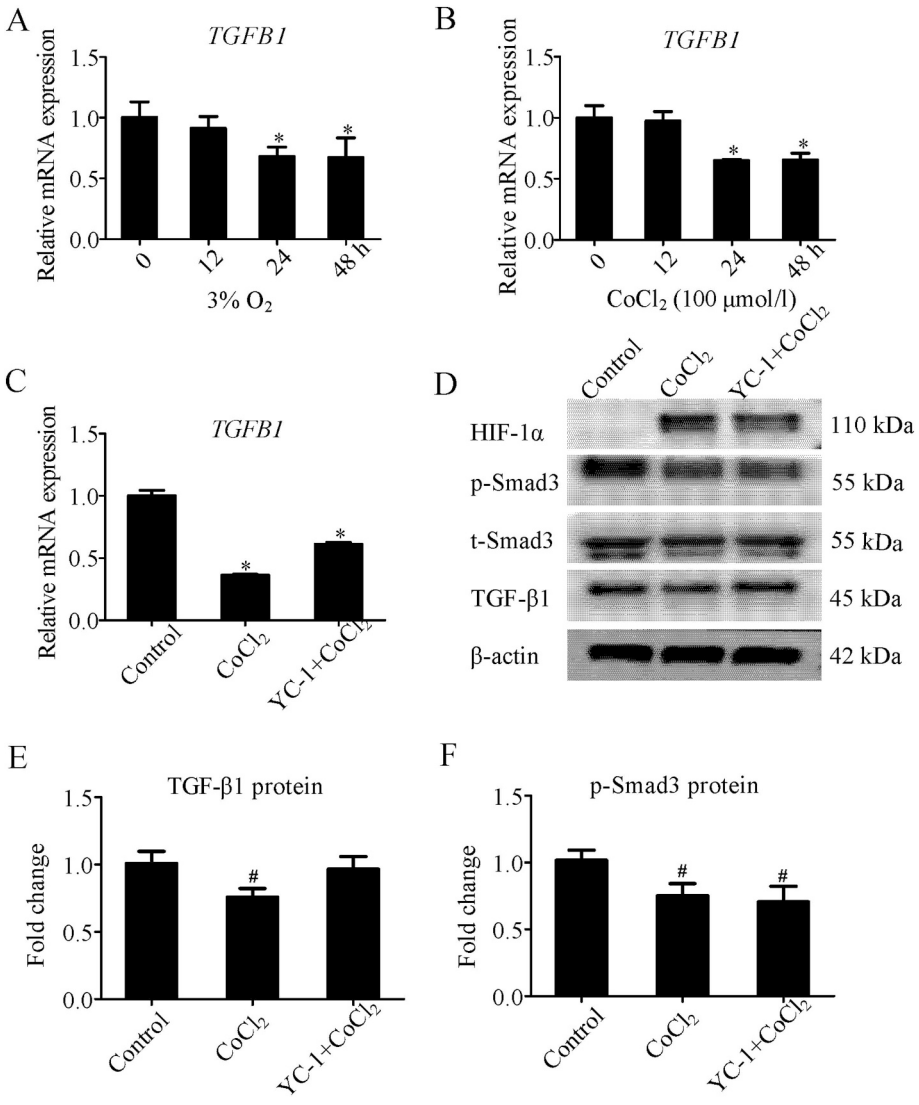

Fig. 4. HIF-1α decreases the expression of TGF-β1 and the phosphorylation of Smad3 in PDLSCs. (A) PDLSCs were cultured in hypoxia (3% O_2) over different time periods (0, 12, 24 and 48 h), and the expression of TGF-β1 mRNA was measured by qPCR. ANOVA coupled with Dunnett's test (2-sided) was used to draw post hoc comparisons. *$p < .05$ versus the control group. (B) After inducing HIF-1α with $CoCl_2$ (100 μmol/l) for different time periods (0, 12, 24 and 48 h) in PDLSCs, the expression of TGF-β1 mRNA was measured by qPCR. ANOVA coupled with Dunnett's test (2-sided) was used to draw post hoc comparisons. *$p < .05$ versus the control group. (C–F) After treating PDLSCs with $CoCl_2$ (100 μmol/l) or $CoCl_2$ with a preceding 5 min of YC-1 (10 μmol/l) for 24 h, the expression of TGF-β1 mRNA and proteins was measured by qPCR and Western blot, respectively. ANOVA coupled with Bonferroni's correction was used to draw post hoc comparisons. *$p < .05$ versus the other groups and $^{\#}p < .05$ versus the control group. Experiments were carried out four times (n = 3). Donor is #9 (male and 14 years of age).

for 10 min with a heat block (Qilinbeier, Haimen, Jiangsu, China). Proteins were then separated by 10% sodium dodecyl sulfate polyacrylamide gel electrophoresis (SDS-PAGE) (components purchased from Solarbio, Beijing, China), transferred onto 0.20 μm polyvinylidene difluoride membranes (Roche, Basel, Switzerland), and blocked by 3% bovine serum albumin (Solarbio, Beijing, China) for 1 h at room temperature. Primary antibody incubation employed rabbit HIF-1α antibody (1:1000, Abcam, Cambridge, UK), rabbit RUNX2 antibody (1:1000, ZEN BIO, Chengdu, Sichuan, UK)rabbit TGF-β1 antibody (1:1000, Bioworld, Saint Louis Park, Minnesota, USA), rabbit Smad3 (phospho-S423) antibody (1:1000, Bioworld, Saint Louis Park, Minnesota, USA), rabbit Smad3 antibody (1:1000, Bioworld, Saint Louis Park, Minnesota, USA), and mouse β-actin antibody (1:1000, Beyotime, Shanghai, China) at 4 °C overnight. Secondary antibody incubation employed peroxidase-conjugated goat anti-rabbit IgG (H + L) (1:10000, Jackson ImmunoResearch Laboratories, West Grove, Pennsylvania, USA) or goat anti-mouse IgG (H + L) (1:5000, Beyotime, Shanghai, China) at room temperature for 1 h. Finally, immunoblot results were visualized via a gel image system (FX5, Vilber Lourmat, Marne-la-Vallée, Paris, France) and an enhanced chemiluminescence detection kit SuperSignal West Femto Maximum Sensitivity Substrate (Thermo Fisher Scientific, Waltham, Massachusetts, USA). The immunoblot results were quantified using Quantity One (4.4.0, Bio-Rad Laboratories, Hercules, California, USA).

2.5. Quantitative polymerase chain reaction

Total RNA was extracted from PDLSCs using TRIzol reagent (Life Technologies, Carlsbad, California, USA) and quantified with a NanoDrop 2000 Spectrophotometer (Thermo Fisher Scientific, Waltham, Massachusetts, USA). Reverse transcription was performed using a Transcriptor First Strand cDNA Synthesis Kit (Basel, Switzerland) and 2720 Thermal Cycler (Life Technologies, Carlsbad, California, USA). qPCR was performed with FastStart Essential DNA Green Master (Roche, Basel, Switzerland) and a LightCycler 96 System (Roche, Basel, Switzerland). All of these steps were performed according to the manufacturers' instructions. Sequences of the primers used were as follows: *HIF1A* forward: CCGCTGGAGACACAATCATA, reverse: GGTGAGGGGA GCATTACATC. *RUNX2* forward: CCTCTGACTTCTGCCTCTGG, reverse: ATGAAATGCTTGGGAACTGC. *TGFB1* forward: GTGGACATCAACGGGT TCACT, reverse: AGTTGGCATGGTAGCCCTTG. *GAPDH* forward: CTCCT CCACCTTTGACGC, reverse CCACCACCCTGTTGCTGT. qPCR results were analyzed using the ΔΔCq method (Cq, quantification cycle) [19].

2.6. Statistical analysis

Immunoblot quantifications and qPCR Cq values were calculated as the means ± standard deviation. IBM SPSS Statistics (25.0, IBM Corporation, Armonk, New York, USA) was used to analyze the quantitative data. One-way analysis of variance (ANOVA) coupled with a Dunnett's test (2-sided)

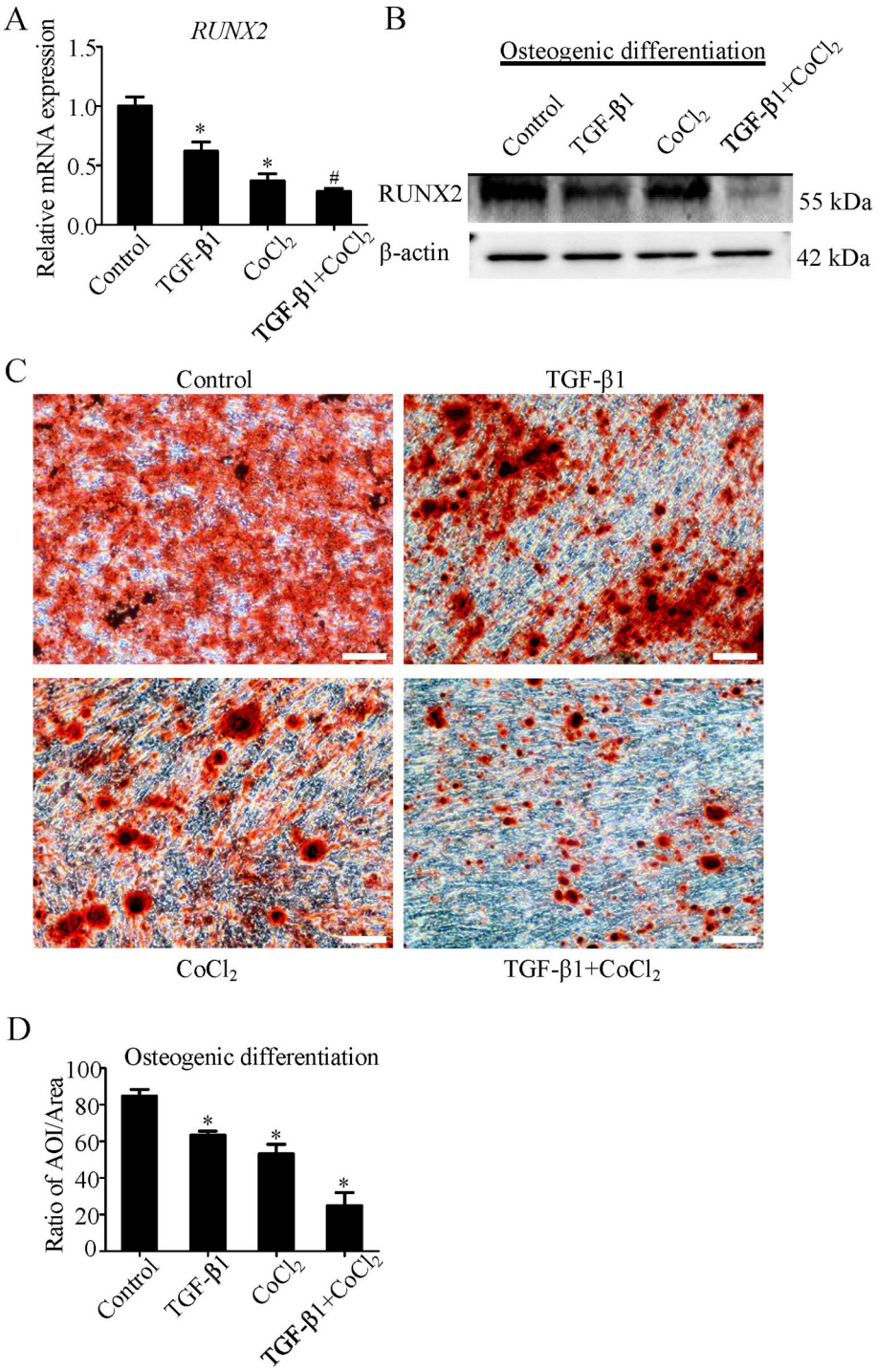

Fig. 5. TGF-β1 and HIF-1α synergistically inhibit the osteogenesis of PDLSCs. (AB) After culturing PDLSCs in osteogenic media with supplements of TGF-β1, $CoCl_2$, or TGF-β1 + $CoCl_2$ for 1 day, RUNX2 mRNA and protein expression was measured by qPCR. ANOVA coupled with Bonferroni's correction was used to draw post hoc comparisons. $^{*}p < .05$ versus the other groups, and $^{\#}p < .05$ versus the control and TGF-β1 groups. Experiments were carried out three times (n = 3). Donor is #9 (male and 14 years of age). (CD) Alizarin Red S staining of the PDLSCs after the osteogenic induction with 2 weeks of TGF-β1, $CoCl_2$, or TGF-β1 + $CoCl_2$ treatment. Red stained mineralization was digitalized by Image-Pro Plus (Media Cybernetics, USA). IOD = Integrated optic density. IOD/Area = mean density. ANOVA coupled with Bonferroni's correction was used to draw post hoc comparisons. $^{*}p < .05$ versus the other groups. Experiments were carried out three times (n = 3). Donor is #2 (female and 13 years of age). (For interpretation of the references to color in this figure legend, the reader is referred to the web version of this article.)

or Bonferroni's correction was used to draw post-hoc comparisons. The Kolmogorov-Smirnov test was used to assess the normal distribution of variables. Levene's test was used to assess the homogeneity of variance. A *P-value* of < 0.05 was considered statistically significant.

3. Results

3.1. Isolation and characterization of PDLSCs

After 3–5 days of culturing, spindle-shaped primary cells emerged from the edges of primary explants and rapidly reached 80% confluence before passing over another 5–7 days (Fig. 1A). By single-cell colony formation assay and crystal violet staining, putative stem cells were preliminarily characterized and screened out (Fig. 1B). Then, the differentiation potential of the putative stem cells was confirmed. Alizarin Red S staining results showed the presence of several red calcified nodules among cells of the osteogenesis group, Oil Red O staining results showed more red fat droplets within cells of the adipogenesis group, and Alcian Blue staining results showed many blue stained matrix in the chondrogenesis group relative to the control group (Fig. 1C). A stem cell surface marker analysis also showed that the isolated cells positively expressed CD44 and CD29, i.e., cell surface markers of MSCs, but negatively expressed CD34 and CD45, i.e., cell surface markers of hematopoietic cells, revealing the origins of these isolated cells (Fig. 1D). In addition, the gene expression of SCX, a specific marker of tendons and PDLSCs, was proved to be expressed more in putative stem cells

isolated from the periodontal ligaments than from adipose-derived stem cells (ADSCs) (Fig. 1E).

3.2. Expression of HIF-1α and TGF-β1 during the osteogenesis of PDLSCs

In carrying out the osteogenic induction of PDLSCs, we found the expression of HIF-1α protein to be significantly enhanced in the later stage (Fig. 2A). This unexpected finding motivated us to explore mechanisms and causes of HIF-1α stabilization during the osteogenesis of PDLSCs. Throughout this process, crucial osteogenic gene *RUNX2* and its protein was found to elevate especially in early stages (Fig. 2B, $p < .05$), and the mRNA expression of the *HIF1A* gene was also observed to increase and peak early on and then decline, before its protein expression (Fig. 2C, $p < .05$). Both the mRNA and protein expression of TGF-β1 increased slowly but significantly throughout the osteogenic progression of PDLSCs (Fig. 2D, $p < .05$).

3.3. TGF-β1 stabilizes HIF-1α expression in normoxia and enhances HIF-1α expression in hypoxia

After 24 h of serum starving, PDLSCs were treated with exogenous human TGF-β1 (0, 1, 5 and 10 ng/ml) for 24 h. The protein levels and mRNA expression of HIF-1α were found to increase drastically and dose-dependently, and 5 ng/ml of TGF-β1 proved sufficient in spurring significant HIF-1α expression (Fig. 3AB, $p < .05$). Thus, 5 ng/ml of TGF-β1 was used in the following experiments. Then, after serum starving the culture for 24 h, PDLSCs were treated with 5 ng/ml of TGF-β1 over different time periods (0, 12 and 24 h), and the time-dependent protein expression and mRNA transcription of HIF-1α was observed (Fig. 3CD, $p < .05$).

When treated with SIS3 (the antagonist of Smad3) at different concentrations (0, 1, 5 and 10 μmol/l) for 24 h after serum starvation, HIF-1α protein levels were significantly reduced, although an obvious reduction of phosphorylated Smad3 was not observed until 10 μmol/l of SIS3 was applied, indicating the sensitivity of effects of TGF-β1/Smad3 signal transduction on HIF-1α. We thus use 10 μmol/l of SIS3 in the following experiments (Fig. 3E). Then, PDLSCs were treated with TGF-β1, SIS3, or TGF-β1 + SIS3 for 24 h after starving the culture, and Western blot and qPCR results confirm that the force elevating mRNA transcription and protein levels of HIF-1α by TGF-β1 was abrogated through SIS3 treatment (Fig. 3FG, $p < .05$).

The effects of TGF-β1 with $CoCl_2$, YC-1 or BAY87–2243 (both the latter two can antagonize the expression of HIF-1α) on the expression of HIF-1α in PDLSCs were also investigated. Compared to TGF-β1, $CoCl_2$ (100 μmol/l) induced the HIF-1α protein to a higher level while TGF-β1 could further enhance the stimulating effects of $CoCl_2$ (Fig. 3H). The administration of both YC-1 (10 μmol/l) and BAY87–2243 (100 μmol/l) did not diminish the basal expression of HIF-1α proteins in normoxia, but could weaken the effects of exogenous TGF-β1 on the stabilization of HIF-1α proteins (Fig. 3IJ).

3.4. HIF-1α decreases the expression of TGF-β1 and the phosphorylation of Smad3 in PDLSCs

We have demonstrated that TGF-β1 can regulate the expression of HIF-1α in PDLSCs, but it is not clear whether HIF-1α may instead regulate the expression of TGF-β1 in PDLSCs. After treating PDLSCs with hypoxia (3% O_2) over different time periods (0, 12, 24 and 48 h), qPCR results revealed that the transcription of *TGFB1* declined after 24 h and continued to decline after 48 h (Fig. 4A, $p < .05$). Then, after inducing the stabilization of HIF-1α with $CoCl_2$ (100 μmol/l), the decreasing *TGFB1* transcription levels by hypoxia observed were confirmed further (Fig. 4B, $p < .05$). The reduction of *TGFB1* transcription levels was relieved when YC-1 was applied prior to $CoCl_2$ treatment (Fig. 4C, $p < .05$). In addition, the protein expression of TGF-β1 and phosphorylated Smad3 was significantly reduced by $CoCl_2$, and the recovery of TGF-β1 expression was observed when YC-1 was added, but phosphorylated Smad3 protein levels were not recovered by inhibiting HIF-1α with YC-1 (Fig. 4D–F, $p < .05$), revealing a more intense feedback effect of HIF-1α on the phosphorylation of Smad3 than on the expression of TGF-β1.

3.5. TGF-β1 and HIF-1α synergistically inhibit the osteogenesis of PDLSCs

To further investigate the effects of TGF-β1 and HIF-1α on the osteogenic differentiation of PDLSCs, cells were cultured in osteogenic media with supplements of TGF-β1, $CoCl_2$, or TGF-β1 + $CoCl_2$. A short period of inducing for one day was used to measure the effects of TGF-β1 and HIF-1α on the initial stage of osteogenesis, and an induction period of two weeks was applied to measure the total effects of TGF-β1 and HIF-1 on final mineralization. As is shown in Fig. 5AB, TGF-β1 induced an evident drop in RUNX2 mRNA and protein expression compared to the control group while after inducing HIF-1α with $CoCl_2$, a greater drop of RUNX2 was observed. Furthermore, the combined administration of TGF-β1 with $CoCl_2$ caused the most significant change in RUNX2 ($p < .05$). Apart from the change observed in crucial osteogenic marker RUNX2, a change in mineralization levels was also detected and the results were digitalized by Image-Pro Plus. The Alizarin Red S staining results show that both TGF-β1 and HIF-1α clearly inhibited the mineralization of PDLSCs, and the combined TGF-β1 and $CoCl_2$ treatment caused the most significant inhibition of PDLSC osteogenesis (Fig. 5CD; $p < .05$).

4. Discussion

This study was driven from an observation that HIF-1α protein expression is enhanced during the ordinary osteogenic differentiation of PDLSCs, which drove us to explore sources and mechanisms of effects of HIF-1α on the osteogenesis of PDLSCs. As TGF-β1 has been proven to be associated with the stabilization of HIF1-α in PDLCs and is closely correlated with osteogenesis progression, it is rational to investigate the roles of TGF-β1 and HIF-1α in the osteogenic differentiation of PDLSCs.

Studies have reported that both TGF-B1 and HIF-1A can either enhance or inhibit osteogenesis. On one hand, TGF-β1 can induce the expression of RUNX2 to inhibit myogenesis and induce osteogenesis with the assistance of bone morphogenetic protein (BMP)-activated Smads in C2C12 pluripotent mesenchymal precursor cells [20], and HIF-1α can facilitate the induction of β-catenin and consistently enhance osteogenesis for human bone marrow-derived mesenchymal stem cells (BMSCs) by inhibiting miR-340-5p [21]. On the other hand, it has been confirmed that TGF-β1 can inhibit osteoblast differentiation indirectly through the activation of β-catenin via ALK-5/Smad3, protein kinase A (PKA), and phosphatidylinositol-3-kinase (PI3K); directly through ALK-5, PKA, and JNK in MSCs [22]; or by upregulating the expression of E3 ubiquitin-protein ligase Smurf1 via ERK signaling in mesenchymal pluripotent cell line C3H10T1/2 [23]. Hypoxia can suppress the osteogenesis of BMSCs through the inactivation of RUNX2 via the ERK1/2 and p38 MAPK signaling pathways [24]. Thus, through different mechanisms, TGF-β1 and HIF-1α can have bilateral effects on the phenotypic expression of osteogenesis as a cell-specific process. However, an HIF-1-independent inhibition of the osteogenesis of ADSCs in hypoxia has been reported [25], indicating the complexity of the role of HIF-1α for the osteogenic differentiation. In this study, we found that both TGF-β1 and HIF-1α can reduce the expression of crucial osteogenic gene *RUNX2* in initial stages of PDLSCS osteogenesis, and they clearly diminish the final mineralization of PDLSCs. In addition, TGF-β1 and HIF-1α can synergistically inhibit the osteogenic differentiation of PDLSCs.

Regarding the interrelationship between TGF-β1 and HIF-1α, some studies have found different regulatory patterns for different cell types. It has been reported that TGF-β1 has no effects on the expression of HIF-1α in liver cancer HepG2 cells [17] or in human umbilical vein endothelial cells [18]. However, in PDLCs and fibroblasts, the stabilization of HIF-1α by TGF-β1 under nonhypoxic conditions was observed [15,16]. In this study, we found that TGF-β1 can induce the stabilization of HIF-1α as part of a dose-dependent and time-dependent pattern found in PDLSCs

under normoxic conditions. Further, consistent with the results of Watanabe et al. [15], after offsetting the efficacy of Smad3 with SIS3, the expression of HIF-1α protein and mRNA was found to be even lower than that observed in normoxia. We also found that TGF-β1 and $CoCl_2$ can synergistically induce the significant expression of HIF-1α while the stabilization of HIF-1α by TGF-β1 is partly counteracted by YC-1 in normoxia. Taken together, our results indicate that TGF-β1 can stabilize HIF-1α in PDLSCs under nonhypoxic conditions via Smad3 and that this stabilization can be enhanced by $CoCl_2$ and partially inhibited by YC-1.

In addition, we found that HIF-1α can interfere with the signal transduction of TGF-β1 by decreasing the expression of TGF-β1 mRNA and protein and by diminishing the phosphorylation of Smad3. However, some studies report inconsistent results. First, hypoxia has been found to activate the TGF-β1/Smad3 signaling pathway in fibroblasts [26], and Hung et al. further confirmed the present of the hypoxia-response element (HRE) in the *TGFB1* promoter by chromatin immunoprecipitation (ChIP) assay in MSC [27]. In addition, it has been demonstrated that TGF-β1 expression undergoes a short-term increase after hypoxia and then gradually declines with the prolonging of hypoxic time in rat mandibular osteoblasts [28]. Thus, it is clear that HIF-1α can induce the expression of TGF-β1 in several types of cells and in different phases of cell growth. However, HIF-1α can also inhibit the expression of TGF-β1. In human fetal osteoblast cells, hypoxia can lead to a decrease in the expression of TGF-β1 [29] consistent with our findings. Yamazaki et al. also report that HIF-1α does not affect the phosphorylation of Smad3 [16], which is inconsistent with our results. Taken together, a reversal of inhibitory signal transduction from HIF-1α to TGF-β1 expression and the phosphorylation of Smad3 indicate the presence of a self-correcting loop between HIF-1α and TGF-β1 in PDLSCs.

In conclusion, we found that TGF-β1 can induce the stabilization of HIF-1α in PDLSCs and that TGF-β1 and HFI-1α can synergistically inhibit the osteogenesis of PDLSCs. In addition, the reversal of negative effects of HIF-1α on the mRNA and protein expression of TGF-β1 and the phosphorylation of Smad3 render regulatory mechanisms between TGF-β1 and HIF-1α in PDLSCs even more complex.

Acknowledgements

The authors would like to thank Dr. Chao Wang (Department of Pediatric Intensive Care Unit, Children's Hospital of Chongqing Medical University, Chongqing 400014, China) for providing us with ADSCs.

Funding

This work was supported by Chongqing State Key Laboratory of Military Stomatology [grant number 2014KA04].

Declaration of competing interest

Declarations of interest: none

References

[1] N.J. Kassebaum, E. Bernabe, M. Dahiya, B. Bhandari, C.J. Murray, W. Marcenes, Global burden of severe periodontitis in 1990-2010: a systematic review and meta-regression, J. Dent. Res. 93 (11) (2014) 1045–1053.

[2] C.J. Smiley, S.L. Tracy, E. Abt, B.S. Michalowicz, M.T. John, J. Gunsolley, C.M. Cobb, J. Rossmann, S.K. Harrel, J.L. Forrest, P.P. Hujoel, K.W. Noraian, H. Greenwell, J. Frantsve-Hawley, C. Estrich, N. Hanson, Systematic review and meta-analysis on the nonsurgical treatment of chronic periodontitis by means of scaling and root planing with or without adjuncts, Journal of the American Dental Association (1939) 146(7) (2015) 508–24.e5.

[3] M. Meimandi, M.R. Talebi Ardakani, A. Esmaeil Nejad, P. Yousefnejad, K. Saebi, M.H. Tayeed, The effect of photodynamic therapy in the treatment of chronic periodontitis: a review of literature, Lasers Med. Sci. 8 (Suppl. 1) (2017) S7–S11.

[4] B.M. Seo, M. Miura, S. Gronthos, P.M. Bartold, S. Batouli, J. Brahim, M. Young, P.G. Robey, C.Y. Wang, S. Shi, Investigation of multipotent postnatal stem cells from human periodontal ligament, Lancet 364 (9429) (2004) 149–155 (London, England).

[5] L. Golz, S. Memmert, B. Rath-Deschner, A. Jager, T. Appel, G. Baumgarten, W. Gotz, S. Frede, Hypoxia and P. gingivalis synergistically induce HIF-1 and NF-kappaB activation in PDL cells and periodontal diseases, Mediat. Inflamm. 2015 (2015) 438085.

[6] N.R. Prabhakar, G.L. Semenza, Oxygen Sensing and Homeostasis, Physiology (Bethesda) 30 (5) (2015) 340–348.

[7] C. Loenarz, M.L. Coleman, A. Boleininger, B. Schierwater, P.W. Holland, P.J. Ratcliffe, C.J. Schofield, The hypoxia-inducible transcription factor pathway regulates oxygen sensing in the simplest animal, Trichoplax adhaerens, EMBO Rep. 12 (1) (2011) 63–70.

[8] G.L. Wang, B.H. Jiang, E.A. Rue, G.L. Semenza, Hypoxia-inducible factor 1 is a basic-helix-loop-helix-PAS heterodimer regulated by cellular O2 tension, Proc. Natl. Acad. Sci. U. S. A. 92 (12) (1995) 5510–5514.

[9] Y. Zhang, J. Huang, C. Wang, Y. Zhang, C. Hu, G. Li, L. Xu, Application of HIF-1alpha by gene therapy enhances angiogenesis and osteogenesis in alveolar bone defect regeneration, The Journal of Gene Medicine 18 (4–6) (2016) 57–64.

[10] L. Li, M.X. Han, S. Li, Y. Xu, L. Wang, Hypoxia regulates the proliferation and osteogenic differentiation of human periodontal ligament cells under cyclic tensile stress via mitogen-activated protein kinase pathways, J. Periodontol. 85 (3) (2014) 498–508.

[11] J.C. Dong, Z.C. Song, R. Shu, S. Li, Z.K. Lin, X.L. Zhang, The effect of hypoxia on proliferation and osteogenic differentiation of periodontal ligament cells, Shanghai kou qiang yi xue = Shanghai journal of stomatology 23 (4) (2014) 397–401.

[12] T. Osathanon, P. Vivatbutsiri, W. Sukarawan, W. Sriarj, P. Pavasant, S. Sooampon, Cobalt chloride supplementation induces stem-cell marker expression and inhibits osteoblastic differentiation in human periodontal ligament cells, Arch. Oral Biol. 60 (1) (2015) 29–36.

[13] G. Semenza, Signal transduction to hypoxia-inducible factor 1, Biochem. Pharmacol. 64 (5–6) (2002) 993–998.

[14] T. Borggrefe, M. Lauth, A. Zwijsen, D. Huylebroeck, F. Oswald, B.D. Giaimo, The notch intracellular domain integrates signals from Wnt, hedgehog, TGFbeta/BMP and hypoxia pathways, Biochim. Biophys. Acta 1863 (2) (2016) 303–313.

[15] T. Watanabe, A. Yasue, E. Tanaka, Inhibition of transforming growth factor beta1/Smad3 signaling decreases hypoxia-inducible factor-1alpha protein stability by inducing prolyl hydroxylase 2 expression in human periodontal ligament cells, J. Periodontol. 84 (9) (2013) 1346–1352.

[16] R. Yamazaki, Y. Kasuya, T. Fujita, H. Umezawa, M. Yanagihara, H. Nakamura, I. Yoshino, K. Tatsumi, T. Murayama, Antifibrotic effects of cyclosporine A on TGF-beta1-treated lung fibroblasts and lungs from bleomycin-treated mice: role of hypoxia-inducible factor-1alpha, FASEB J. 31 (8) (2017) 3359–3371.

[17] X.H. Wang, M.N. Liu, X. Sun, C.H. Xu, J. Liu, J. Chen, R.L. Xu, B.X. Li, TGF-beta1 pathway affects the protein expression of many signaling pathways, markers of liver cancer stem cells, cytokeratins, and TERT in liver cancer HepG2 cells, Tumour Biol. 37 (3) (2016) 3675–3681.

[18] H. Sui, J. Zhao, L. Zhou, H. Wen, W. Deng, C. Li, Q. Ji, X. Liu, Y. Feng, N. Chai, Q. Zhang, J. Cai, Q. Li, Tanshinone IIA inhibits beta-catenin/VEGF-mediated angiogenesis by targeting TGF-beta1 in normoxic and HIF-1alpha in hypoxic microenvironments in human colorectal cancer, Cancer Lett. 403 (2017) 86–97.

[19] K.J. Livak, T.D. Schmittgen, Analysis of relative gene expression data using real-time quantitative PCR and the 2(−Delta Delta C(T)) method, Methods 25 (4) (2001) 402–408.

[20] S.C. Bae, K.S. Lee, Y.W. Zhang, Y. Ito, Intimate relationship between TGF-beta/BMP signaling and runt domain transcription factor, PEBP2/CBF, J. Bone Joint Surg.. American volume 83-A Suppl 1(Pt 1) (2001) S48–55.

[21] K. Du, Z. Li, X. Fang, T. Cao, Y. Xu, Ferulic acid promotes osteogenesis of bone marrow-derived mesenchymal stem cells by inhibiting microRNA-340 to induce beta-catenin expression through hypoxia, Eur. J. Cell Biol. 96 (6) (2017) 496–503.

[22] S. Zhou, TGF-beta regulates beta-catenin signaling and osteoblast differentiation in human mesenchymal stem cells, J. Cell. Biochem. 112 (6) (2011) 1651–1660.

[23] X. Sun, Z. Xie, Y. Ma, X. Pan, J. Wang, Z. Chen, P. Shi, TGF-beta inhibits osteogenesis by upregulating the expression of ubiquitin ligase SMURF1 via MAPK-ERK signaling, J. Cell. Physiol. 233 (1) (2018) 596–606.

[24] P. Zhang, N. Ha, Q. Dai, S. Zhou, C. Yu, L. Jiang, Hypoxia suppresses osteogenesis of bone mesenchymal stem cells via the extracellular signalregulated 1/2 and p38mitogen activated protein kinase signaling pathways, Mol. Med. Rep. 16 (4) (2017) 5515–5522.

[25] S. Sahai, A. Williams, M.L. Skiles, J.O. Blanchette, Osteogenic differentiation of adipose-derived stem cells is hypoxia-inducible factor-1 independent, Tissue Eng. A 19 (13–14) (2013) 1583–1591.

[26] B. Zhao, H. Guan, J.Q. Liu, Z. Zheng, Q. Zhou, J. Zhang, L.L. Su, D.H. Hu, Hypoxia drives the transition of human dermal fibroblasts to a myofibroblast-like phenotype via the TGF-beta1/Smad3 pathway, Int. J. Mol. Med. 39 (1) (2017) 153–159.

[27] S.P. Hung, M.H. Yang, K.F. Tseng, O.K. Lee, Hypoxia-induced secretion of TGF-beta1 in mesenchymal stem cell promotes breast cancer cell progression, Cell Transplant. 22 (10) (2013) 1869–1882.

[28] J. Guan, J. Wang, X. Che, D. Li, Experimental study on the effect of hypoxia on the expression of VEGF and TGF-beta1 of rat mandibular osteoblasts, Zhongguo Xiu Fu Chong Jian Wai Ke Za Zhi = Zhongguo Xiufu Chongjian Waike Zazhi = Chinese Journal of Reparative and Reconstructive Surgery 22 (8) (2008) 984–988.

[29] S.J. Pyo, W.W. Song, I.R. Kim, B.S. Park, C.H. Kim, S.H. Shin, I.K. Chung, Y.D. Kim, Low-level laser therapy induces the expressions of BMP-2, osteocalcin, and TGF-beta1 in hypoxic-cultured human osteoblasts, Lasers Med. Sci. 28 (2) (2013) 543–550.